Hybrid S-Transform and Kalman Filtering Approach for Detection and Measurement of Short Duration Disturbances in Power Networks

P. K. Dash, *Senior Member, IEEE,* and M. V. Chilukuri, *Member, IEEE*

***Abstract*—This paper presents a new approach in the detection, localization, and classification of short duration disturbances in the power networks using a phase-corrected wavelet transform known as S-transform (ST) and an extended Kalman filter (EKF). The ST has excellent time-frequency resolution characteristics and provides detection, localization, and visual patterns suitable for automatic recognition of power quality events. The EKF, on the other hand, provides automatic classification and measurements of the frequently occurring power frequency short duration disturbances on the power networks. Thus, by combining both the ST and EKF, it is possible to completely classify and measure the short duration power quality disturbances. The proposed technique is applied to both simulated and experimentally obtained short duration power network disturbances in the presence of additive noise, and the results reveal significant accuracy in completely characterizing the power quality events.**

***Index Terms*—Extended complex Kalman filter (ECKF), frequency estimation, noise rejection, S-transform (ST), short duration disturbance (SDD), time-frequency localization.**

I. Introduction

IN THIS PAPER, we propose a novel digital signal processing technique for the detection, classification and measurement of frequently occurring short duration disturbances (SDD) in the power networks, which are usually contaminated with noise. The disturbance occurring in the electric supply network is a major issue in manufacturing industries and causes very expensive consequences. These disturbances are primarily due to the use of nonlinear loads, power electronics equipment, and unbalanced loads. A recent survey attributes that 92% of power quality disturbances are voltage sags [14]. It has been reported that an interruption in the electric network or 30% voltage sag or swell for a very short duration (three to four cycles) can reset programmable controllers (PLC) for the entire assembly line. Such disturbances should be detected and classified accurately so that control action can be initiated. The proposed paper is an attempt in this direction to improve power quality in distribution networks.

The past 20 years have heralded major improvements in the field of signal analysis, along with the development of mathematics and signal processing [1]. These new developments provide high-performance signal analysis because they employ more understandable signal representations than time or frequency representation of signals. These potential tools have been successfully applied in geophysics, acoustics, image processing, data compression, and, recently, power quality analysis [2]–[5]. Several techniques, leading to time-frequency representation and applicable to SDD, are investigated here.

To analyze a distorted signal, a discrete short time Fourier transform (STFT) is most often used. This transform performs satisfactorily for stationary signals where properties of signals do not change with time. For nonstationary signals, the STFT does not track the signal dynamics properly. On the other hand, the wavelet analysis provides a unified framework for processing distorted signals. Wavelet analysis [6] is based on the decomposition of a signal according to time-scale, rather than frequency, using basis functions with adaptable scaling properties; this is known as multiresolution analysis. A wavelet transform (WT) expands a signal not in terms of a trigonometric polynomial but by wavelets, generated using transition (shift in time) and dilation (compression in time) of a fixed wavelet function called the "mother wavelet." The wavelet function is localized both in time and frequency, yielding wavelet coefficients at different scales. This gives the WT much greater compact support for analysis of signals with localized transient components arising in power quality disturbances. Several types of wavelets have been considered [7]–[9] for detection, localization, and classification of power quality problems as both time and frequency information is available by multiresolution analysis. At first, the extraction of the occurred disturbance requires its time duration estimation. This information is vital as there is a need to obtain the sampling frequency and the frequency subband containing most of the spectral energy. However, this process is very much influenced by the noise superimposed on the signal and the iterative nature of the wavelet transform-based algorithms requiring different sampling frequencies for different frequency subbands.

The S-transform (ST) [10], on the other hand, is an extension to the ideas of WT, and is based on a moving and scalable localizing Gaussian window and has characteristics superior to either of the transforms. The ST is fully convertible from the time domain to two-dimensional (2-D) frequency translation domain and then to familiar Fourier frequency domain. The amplitude—frequency—time spectrum and the phase—frequency—time spectrum are both useful in defining local spectral characteristics. The superior properties of the ST are due to the fact that the modulating sinusoids are fixed with respect to the time axis, while the localizing scalable Gaussian

Manuscript received August 27, 2001; revised August 12, 2003.
P. K. Dash is with the Silicon Institute of Technology, Bhubaneswar, India.
M. V. Chilukuri is with the Multimedia University, Cyberjaya 63100, Malaysia.
Digital Object Identifier 10.1109/TIM.2003.820486

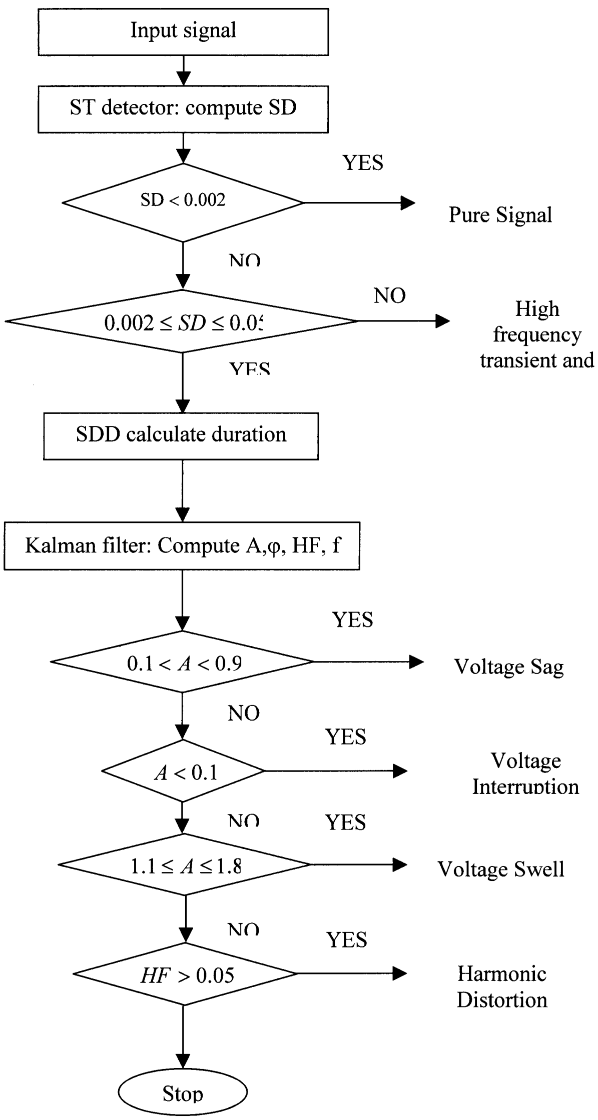

Fig. 1. Hybrid ST Kalman filter.

window dilates and translates. As a result, the phase spectrum is absolute in the sense that it always refers to the origin of the time axis. The real and imaginary spectrum can be localized independently with a resolution in time corresponding to the basis function in question, and the changes in the absolute phase of a constituent frequency can be followed along the time axis. The phase information associated with the ST makes it an ideal candidate for the detection and classification of nonstationary signals.

Among the several numerical techniques, Kalman filtering [11], [12] approaches have attracted widespread attention, as they accurately estimate the amplitude, phase and frequency of a signal contaminated with noise and harmonics. In this paper, a variation of the nonlinear Kalman filter [13] is presented which simplifies the modeling requirement for amplitude and frequency estimation of a signal.

The ST matrix of the SDD signal is computed, and it is used to detect, localize, and visually classify the SDD. Then, the short duration distorted part of the signal is fed to a Kalman filter to estimate the amplitude, frequency, and harmonic contents to provide automatic recognition and measurement of the disturbance. Extensive computer simulation and laboratory tests are performed to validate the efficacy of the proposed approach.

II. S-Transform (ST)

A. Basic Principles

The ST is an extension to the Gabor transform and WT and falls within the broad range of multiresolution spectral analysis, used with a translatable and scalable Gaussian window, where the standard deviation is an inverse function of the frequency, thus reducing the dimension of the transform. With the introduction of a dilation parameter, the localizing Gaussian function $\mathrm{g}(t)$ is defined as

$$g(t) = \frac{1}{\sigma\sqrt{2\pi}} e^{-[\frac{t^2}{2\sigma^2}]} \tag{1}$$

where σ is the standard deviation. The Multiresolution ST is defined by

$$\mathrm{S}(f,\tau,\sigma) = \int_{-\infty}^{\infty} h(t) g(\tau - t, \sigma) e^{-i2\pi f t} dt. \tag{2}$$

This falls within the definition of the multiresolution Fourier transform. The Gabor transform $\Gamma(f,\tau)$ is a particular case of $\mathrm{S}(f,\tau,\sigma)$ with σ held constant. The primary purpose of the dilation (or scaling) parameter is to increase the width of the window function $\mathrm{g}(t,\sigma)$ for lower frequency and vise versa, and is controlled by selecting a specific functional dependency of σ with the frequency f. The ST performs multiresolution analysis on the signal, because the width of its window varies inversely with the frequency. This gives high time resolution at high frequencies and high frequency resolutions at low frequencies. We have chosen the width of the window to be proportional to the period of the cosinusoid being localized

$$\sigma(f) = T = \frac{k}{|f|} \tag{3}$$

where T is the time period. The choice of unity for the constant k in (3) makes the Gaussian window in (1) the narrowest in the time domain. The ST may be written as

$$\mathrm{S}(f,\tau) = \int_{-\infty}^{\infty} h(t) \times \frac{|f|}{\sqrt{2\pi}} e^{-\frac{(\tau-t)^2 f^2}{2}} \times e^{-i2\pi f t} dt \tag{4}$$

One can see here that the zero frequency of the ST is identically equal to zero for this definition of $\sigma(f)$. This adds no information. Therefore, $\mathrm{S}(f,\tau)$ is defined as independent of time and is equal to the average of the function $h(t)$, i.e.

$$\mathrm{S}(0,\tau) = \lim_{\mathrm{T}\to\infty} \frac{1}{T} \int_{-\frac{T}{2}}^{\frac{T}{2}} h(t)\, dt. \tag{5}$$

For the discrete ST, $h(t)$ can be written in discrete form as $h[pT]$, where p varies from 0 to $\mathrm{N}-1$ and is known as discrete

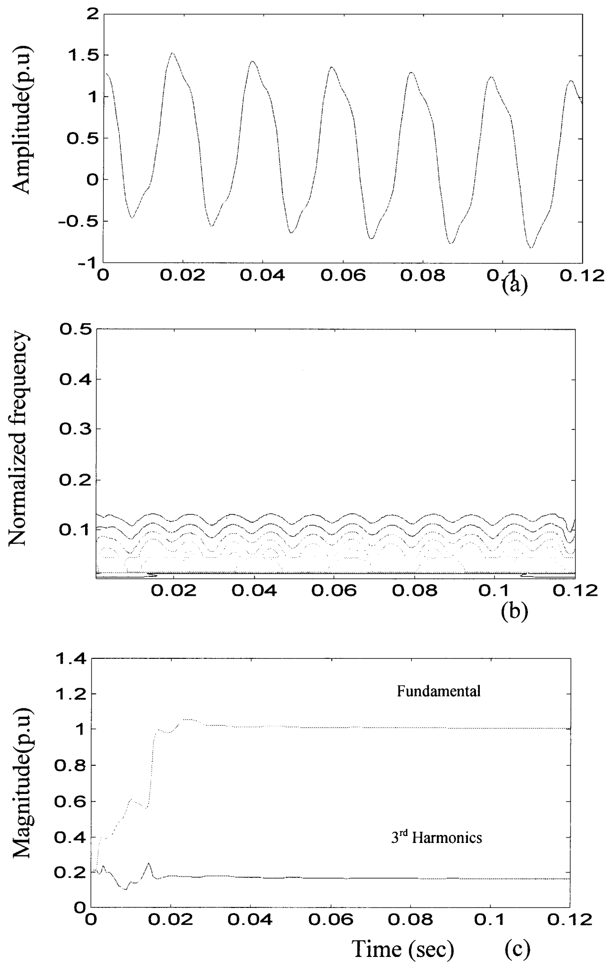

Fig. 2. (a) Example of a 50-Hz signal with 16% of third harmonics. (b) S Transform contour plot. (c) Estimated amplitude plot.

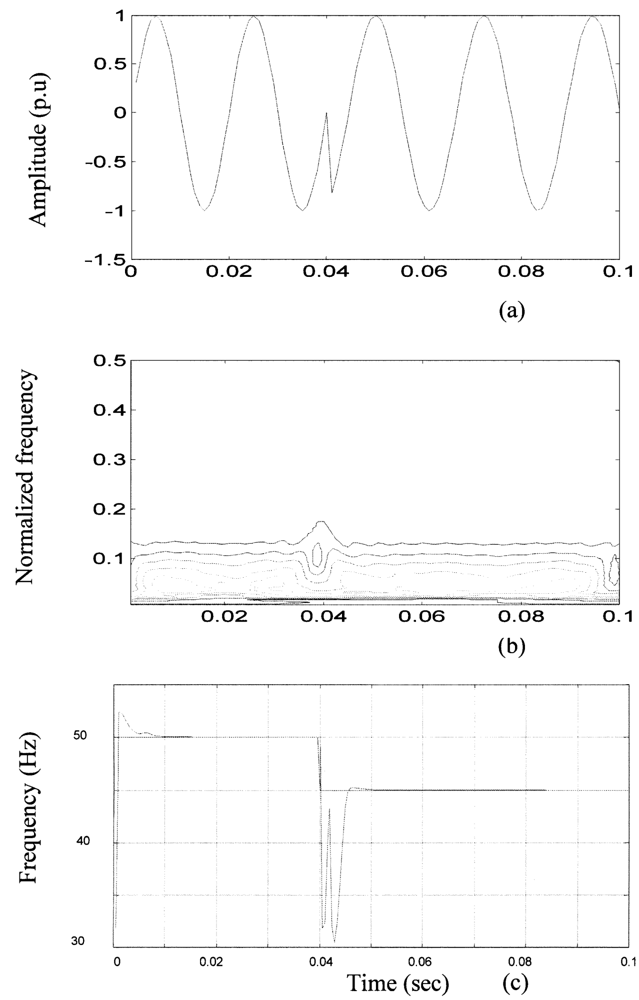

Fig. 3. (a) Example of sudden frequency change. (b) ST contour plot. (c) Estimated frequency plot.

time series of the signal h(t). Discrete Fourier transform of the time series $h[pT]$ can be expressed as

$$H\left[\frac{n}{NT}\right] = \frac{1}{N}\sum_{p=0}^{N-1} h[pT]e^{-\frac{i2\pi nk}{N}} \tag{6}$$

where $n = 0, 1, \ldots, N-1$ and the inverse discrete Fourier transform is

$$h[pT] = \sum_{n=0}^{N-1} H\left[\frac{n}{NT}\right] e^{i\frac{2\pi nk}{N}}. \tag{7}$$

The ST in discrete case is the projection of the vector defined by the time series $h[pT]$ onto a spanning set of vectors. Since spanning vectors are not orthogonal and the elements of S matrix are not dependent, each basis vector is divided into N localized vectors by an element by element product with N shifted Gaussians, such that sum of these N localized vectors is the original basis vector. The ST of the discrete time series $h[pT]$ is given by

$$S\left[\frac{n}{NT}, jT\right] = \sum_{m=0}^{N-1} H\left[\frac{m+n}{NT}\right] e^{-\frac{2\pi^2 m^2}{n^2}} e^{i\frac{2\pi m j}{N}}. \tag{8}$$

For $n = 0$

$$S[0, jT] = \frac{1}{N}\sum_{m=0}^{N-1} h\left[\frac{m}{NT}\right] \tag{9}$$

where j, m, and $n = 0, 1, \ldots, N-1$.

B. Implementation of ST

The computation of the ST is efficiently implemented using the convolution theorem and FFT. The following steps are used for the computation of ST.

i) Denote $n/NT, m/NT, kT$, and jT as n, m, k, and j, respectively, for the evaluation of ST.
ii) Compute the DFT of the signal $h(k)$ using FFT software routine and shift spectrum $H[m]$ to $H[m+n]$.
iii) Compute the Gaussian window function $\exp(-2\pi^2\, m^2/n^2)$ for the required frequency n.
iv) Compute the inverse Fourier transform of the product of DFT and Gaussian window function to give the ST matrix.

The output of the ST is an $n \times m$ matrix, whose rows pertain to frequency and columns indicate time. Each column thus represents the "local spectrum" for that point in time. From the

TABLE I
STANDARD DEVIATION AND HARMONIC FACTOR

Features	Voltage Interruption without Noise									
Voltage Amplitude	0.01	0.02	0.03	0.04	0.05	0.06	0.07	0.08	0.09	0.1
A	0.0186	0.0295	0.038	0.048	0.055	0.0662	0.0703	0.803	0.903	1.1003
SD	0.0367	0.0364	0.0362	0.0361	0.0356	0.0355	0.0354	0.0349	0.0348	0.0348
HF	0.012	0.0125	0.0131	0.131	0.0135	0.0136	0.0138	0.0139	0.0138	0.0139
	Voltage Interruption With 30 dB noise									
A	0.0752	0.076	0.075	0.072		0.0704	0.0724	0.0858	0.0878	0.0975
SD	0.0350	0.0370	0.0358	0.0348	0.0387	0.0346	0.0360	0.0350	0.0342	0.0343
HF	0.039	0.037	0.038	0.038	0.037	0.034	0.035	0.0343	0.0338	0.0346

TABLE II
STANDARD DEVIATION AND HARMONIC FACTOR

Features	Voltage Sag and Swell without noise								
Sag & Swell (Actual)	0.2	0.4	0.6	0.8	1	1.2	1.4	1.6	1.8
A	0.2003	0.4002	0.6001	0.8002	1	1.201	1.403	1.605	1.806
SD	0.0317	0.017	0.010	0.008	0	0.005	0.0106	0.0159	0.024
HF	0.0384	0.338	0.0168	0.0247	0	0.007	0.0132	0.0173	0.0206
	Voltage Sag and Swell with 30 dB noise								
A	0.2073	0.4029	0.5918	0.798	0.997	1.192	1.399	1.598	1.793
SD	0.0278	0.0207	0.0223	0.0055	0	0.0056	0.0106	0.0156	0.0226
HF	0.0384	0.0338	0.0275	0.0247	0.028	0.0275	0.0309	0.0268	0.0308

TABLE III
STANDARD DEVIATION AND HARMONIC FACTOR

Features	Normal Voltage + Harmonics with Noise					
Harmonic Values	2.5%	5%	8%	10%	15%	20%
Voltage Magnitude	1.0	1.0	1.0	1.0	1.0	1.0
A	1.006	0.994	1.006	1.005	0.998	0.997
SD	0.0044	0.0106	0.0256	0.0339	0.046	0.056
HF	0.0353	0.0707	0.113	0.141	0.212	0.28

ST matrix, we obtain the frequency-time contours having the same amplitude spectrum and these contours can be used to visually classify the nature of the disturbance event. However, for automatic classification of the disturbances, the standard deviation (SD) of the most significant contour having the largest frequency amplitude versus time is calculated. Thus SD = std (contour c1) and it can be considered as a measure of the energy of the signal with zero mean. The standard deviation of the disturbance signal is found to indicate whether the signal belongs to normal class or the disturbed one. Further, it can be used to distinguish between short duration power frequency disturbances or high frequency oscillatory transients. Once the signal is found to contain a disturbance the next step is to compute its duration and use the extended Kalman filter (EKF) for the estimation of amplitude, frequency, phase, and the harmonic content during the distortion. The next section describes an EKF for the computation of the above quantities, which can be used for further classification of the nature of the disturbance, that is, whether it is a voltage sag, or voltage swell or interruption.

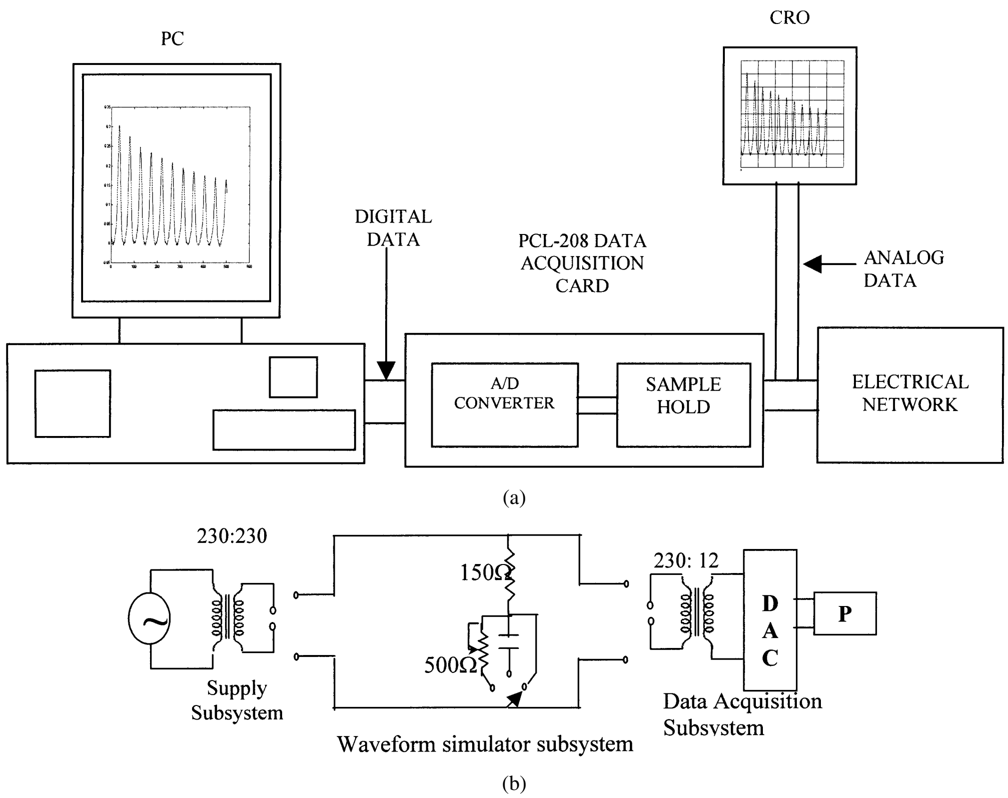

Fig. 4 (a) Experimental setup. (b) Laboratory setup for simulation of sag, swell, and momentary interruption.

III. EXTENDED KALMAN FILTER

Detection, measurement, and classification are the three important aspects for power quality analysis, where as ST or WT can only detect and classify the distorted signals. Several methods are already developed for the measurement of percentage change in amplitude, frequency, and the harmonic content of the distorted signal [11]–[13]. Out of all the approaches, the Kalman filtering approach is the best one. The important fact about the Kalman filtering approach is that it can perfectly track the percentage change in amplitude, frequency, and the harmonic content of the abnormal power signal in the presence of noise [13]. Taking this advantage into consideration, in this paper, we have implemented Kalman filter approach for classification and measurement purpose. The fundamental principle of Kalman Filter approach is described below.

The discrete values of the voltage signals of a power network are transformed into a complex vector using the well-known $\alpha\beta$-transform used in power system analysis. This complex voltage vector is then modeled along with frequency in a nonlinear state-space form and the theory of extended Kalman filter is used to obtain the state vectors iteratively. The computation of Kalman gain and choice of initial covariance matrix are crucial in determining the speed of convergence of the new algorithm and its noise rejection property. The characteristic of the model is that only two states are required to extract the signal frequency with the extended complex Kalman filtering (ECKF). A variety of simulated power network conditions are used for the application of this new technique.

The discrete representation of three phase voltages of a power network is obtained as

$$\begin{aligned} V_{a_k} &= V_m \cos(\omega k \Delta T + \phi) + \in_{a_k} \\ V_{b_k} &= V_m \cos(\omega k \Delta T + \phi - 2\pi/3) + \in_{b_k} \\ V_{c_k} &= V_m \cos(\omega k \Delta T + \phi + 2\pi/3) + \in_{c_k} \end{aligned} \quad (10)$$

where V_m is the peak value of the fundamental component, $\in_{a_k}$, $\in_{b_k}$, and $\in_{c_k}$ are noise terms that can be any combination of white noise and harmonics, ΔT is the sampling interval, k is the sampling instant (iteration count), ϕ is the phase fundamental component, and ω is the angular frequency of the voltage signal ($\omega = 2\pi f_r$, f_r being the system frequency). The $\alpha - \beta$ components are obtained from the above discrete phase voltages as

$$\begin{bmatrix} V_{\alpha_k} \\ V_{\beta_k} \end{bmatrix} = \sqrt{\frac{2}{3}} \begin{bmatrix} 1 & -\frac{1}{2} & -\frac{1}{2} \\ 0 & \frac{\sqrt{3}}{2} & -\frac{\sqrt{3}}{2} \end{bmatrix} \begin{bmatrix} V_{a_k} \\ V_{b_k} \\ V_{c_k} \end{bmatrix}. \quad (11)$$

A complex voltage V_k is obtained from (11) as

$$V_k = V_{\alpha_k} + jV_{\beta_k} = Ae^{j(\omega k \Delta T + \phi)} + \xi_k \quad (12)$$

where A is amplitude of the signal V_k and ξ_k is its noise component.

The discrete observation signal V_k can now be modeled in a state-space form as

$$\begin{bmatrix} x_{1_{k+1}} \\ x_{2_{k+1}} \end{bmatrix} = \begin{bmatrix} 1 & 0 \\ 0 & x_{1_k} \end{bmatrix} \begin{bmatrix} x_{1_k} \\ x_{2_k} \end{bmatrix}. \quad (13)$$

The measurement model becomes

$$y_k = V_k = [0 \quad 1] \begin{bmatrix} x_{1_k} \\ x_{2_k} \end{bmatrix} + \xi_k \tag{14}$$

where the states x_1 and x_2 are

$$\begin{aligned} x_{1_k} &= e^{j\omega\Delta T} = \cos\omega\Delta T + j\sin\omega\Delta T \\ x_{2_k} &= Ae^{j(\omega k\Delta T+\phi)} \end{aligned} \tag{15}$$

and $\Delta T =$ sampling interval.

The above linear stochastic filter is also equivalent to the following nonlinear one

$$x_{k+1} = f(x_k) \quad \text{and} \quad y_k = h(x_k) + \eta_k \tag{16}$$

where

$$\mathrm{x_k} = [\mathrm{x_{1_k}} \quad \mathrm{x_{2_k}}]^{\mathrm{T}} \quad \text{and} \quad f(x_{\mathrm{k}}) = [\mathrm{x_{1_k}} \quad \mathrm{x_{1_k}x_{2_k}}]^{\mathrm{T}}. \tag{17}$$

The observation matrix is obtained as

$$H = \frac{\partial h(x_k)}{\partial x_k} = [0 \quad 1]$$
$$f(\,) = \text{a nonlinear function}$$

The ECKF is applied to the linear system described in (16). The ECKF measurement update equations are

$$K_k = \hat{P}_{(k/k-1)}H^{*T}\left[H\hat{P}_{(k/k-1)}H^{*T} + R\right]^{-1} \tag{18}$$

$$\hat{x}_{k/k} = \hat{x}_{(k/k-1)} + K_k\left(y_k - H\hat{x}_{(k/k-1)}\right) \tag{19}$$

$$\hat{P}_{k/k} = \hat{P}_{k/k-1} - K_kH\hat{P}_{k/k-1} \tag{20}$$

and the time update equations are

$$\hat{x}_{(k+1/k)} = f(\hat{x}_{k/k}) \tag{21}$$

$$\hat{P}_{k+1/k} = F_k\hat{P}_{k/k}F_k^{*T} \tag{22}$$

where

$$F_k = \left.\frac{\partial f(x_k)}{\partial x_k}\right|_{x_k=\hat{x}_{(k/k)}} = \begin{bmatrix} 1 & 0 \\ \hat{x}_{2_{k/k}} & \hat{x}_{1_{k/k}} \end{bmatrix} \tag{23}$$

and $K_k =$ Kalman gain matrix.

$\hat{P}_{k/k}$ or $\hat{P}_{(k+1/k)} =$ Covariance matrix, $R =$ measurement noise variance, $H =$ Observation vector$^*, T$ represent conjugate and transpose of a complex quantity, respectively.

In the above formulation, the state-space representation given in (13) can be expanded to include decaying dc and harmonic components if necessary. For example, if there is a fifth harmonic (x_5) in the signal, the state-space model becomes

$$\begin{bmatrix} x_{1_k} \\ x_{2_k} \\ x_{3_k} \end{bmatrix} = \begin{bmatrix} 1 & 0 & 0 \\ 0 & x_{1_k} & 0 \\ 0 & 0 & x_{1_k}^5 \end{bmatrix} \begin{bmatrix} x_{1_k} \\ x_{2_k} \\ x_{3_k} \end{bmatrix}. \tag{24}$$

The decaying dc component, $V_{\mathrm{dc}}e^{-\alpha_{\mathrm{dc}}t}$ (where V_{dc} and α_{dc} are decaying dc amplitude and decay rate, respectively) is modeled as

$$\begin{aligned} x_{4_k} &= e^{-\alpha_{\mathrm{dc}}\Delta T} \\ x_{5_k} &= V_{\mathrm{dc}}e^{-\alpha_{\mathrm{dc}}k\Delta T} \\ x_{4_{k+1}} &= x_{4_k} \quad \text{and} \quad x_{5_{k+1}} = x_{4_k}x_{5_k}. \end{aligned} \tag{25}$$

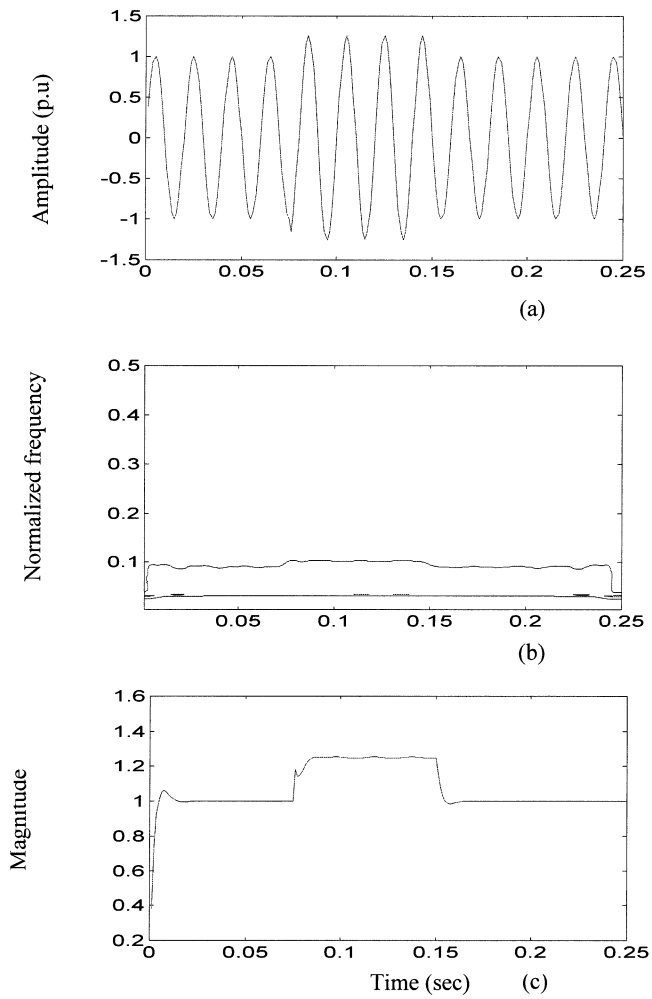

Fig. 5. (a) Example of 25% voltage swell. (b) ST contour plot. (c) Estimated amplitude.

This nonlinear filter is quite stable regardless of the initial conditions of the states x_1 and x_2, provided the observation signal is bounded, which is usually true in a practical system like the power system. After the convergence of the state vector is attained, the frequency is calculated as

$$\hat{f}_k = \frac{1}{2\pi\Delta T}\sin^{-1}\left[\mathrm{Im}\left(\hat{x}_{1_k}\right)\right] \tag{26}$$

where $\mathrm{Im}(\,)$ stands for the imaginary part of a quantity.

Further, the amplitude of the signal A can be obtained from

$$A = |x_2|. \tag{27}$$

IV. Computational and Experimental Test Results

Fig. 1 shows a Hybrid ST and Kalman filtering approach to classify and measure the changes in amplitude and frequency of the pure sinusoidal signal in distorted environment. Different cases of sag, swell, momentary interruption, and frequency change are tested using this approach. Test 1 analyzes different types of major power quality problems, such as sudden frequency change and harmonic distorted signal, using simulated waveforms using MATLAB software package. Test 2 analyzes distorted signal generated using experimental setup. The

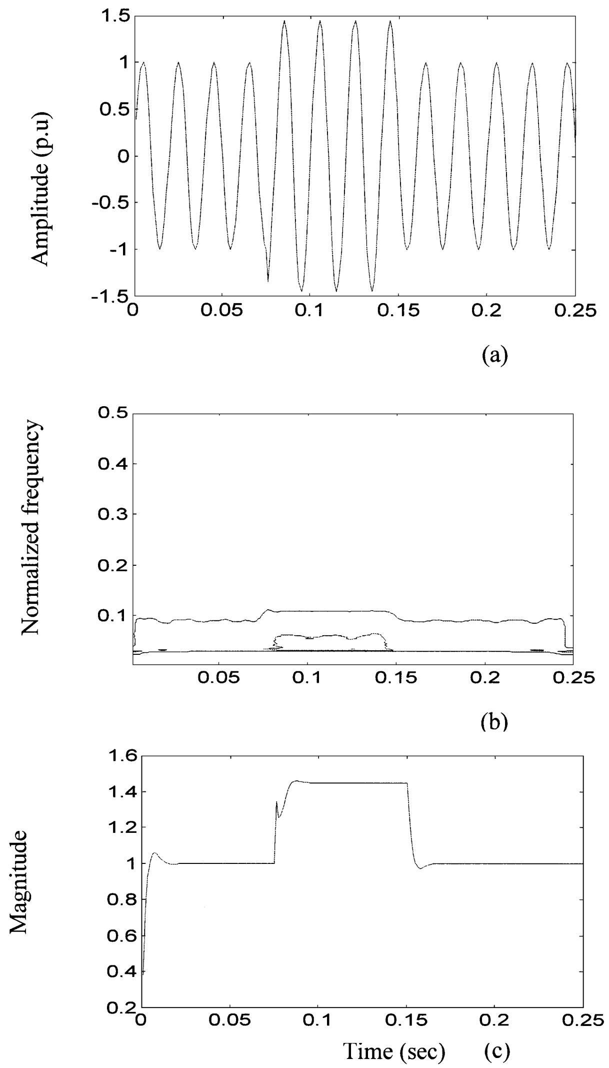

Fig. 6. (a) Example of 45% voltage swell. (b) ST contour plot. (c) Estimated amplitude.

chosen sampling rate is 2.5 kHz, for Test 1 and 2.3 kHz for Test 2, and the frequency (f) is normalized with respect to a base frequency. The ST output shows the plot of the amplitude contours of a given magnitude in the time-frequency coordinate system. The SD of the contour number 1(having the largest frequency amplitude variation with time) is computed and used to detect the presence of disturbance and its duration is calculated from the change in frequency amplitude of the contour number 1. Further SD indicates whether the disturbance is a steady state short duration disturbance or other high frequency phenomenon. The flow chart shown in Fig. 1 clearly indicates that after detection and localization, the EKF is used to classify and estimate the parameters of the disturbance signal. Fig. 1 shows the flow chart of the hybrid detection and estimation algorithm. The following sections provide computational and experimental results.

1) Test 1: Computational Results: To illustrate the application of the hybrid approach, the following case studies are presented.

a) Harmonic Distortion: A fundamental sine wave voltage signal is superimposed with a 16% third harmonic component and the ST contour is computed and plotted for this distorted signal. Fig. 2 shows the original distorted signal and the corresponding ST output contour. This figure also presents the Kalman filter output where both the fundamental and third harmonic components are shown. The standard deviation of the distorted signal is found to be SD $= 0.0228$ and the harmonic factor (HF) is computed as HF $= 0.159$. With the logic presented in the flow chart (Fig. 1), the distorted signal is identified to have third harmonic distortion of 15.9% in comparison to the fundamental.

b) Sudden Frequency Change: Fig. 3(a) shows the waveform, when the frequency is suddenly reduced from 50 Hz to 45 Hz. Such a distorted signal is analyzed by the present approach and the results are plotted as in Figs. 6(b) and (c), respectively. The frequency distortion is reflected in the magnitude of the standard deviation SD which increases from zero to 0.087, and the harmonic factor HF $= 0.0285$. For this frequency change, the time-frequency curve shows localized contours, which provide an excellent visual classification. However, with SD > 0.05, the waveform is identified to belong to a class other than voltage sag, voltage swell, or interruption. The Kalman filter accurately tracks the amplitude of the frequency changes of the original 50-Hz signal.

c) Standard Deviation of Short Duration Disturbances: Several typical short duration power network disturbances like voltage sag, voltage swell, harmonics, and voltage interruption are simulated and the standard deviation SD of the contour no. 1 is evaluated in each case. Tables I–III show this value along with amplitude A, and harmonic factor HF for different magnitudes of sag, swell, and interruption, with or without noise. Here, the signal to noise ratio (SNR) is taken as 30 dB, which is approximately 3.5% of the signal amplitude. Further, the maximum amplitude of the third and fifth harmonic components of the signal is limited to 20% of the fundamental. The presence of sub harmonics and higher frequency harmonics in the signal does not affect substantially in the detection, localization, and classification of the disturbance as their amplitudes are usually very small and they can be treated as noise components.

2) Test 2: Experimental Setup: Experimental test data is generated using practical setup, as shown in Fig. 4(a). Then, both the signal-processing techniques are applied to the acquired signals. The sampling rate is chosen as 2.3 kHz. The following case studies are presented in this paper to evaluate the performance of the above approach. Different power quality signals like sag, swell, and momentary interruption are obtained from the experiment conducted in the laboratory. Fig. 4(b) shows the practical setup to obtained sag, swell and momentary interruption signals. The load is fed from a 3 kVA, 230:230 single-phase transformer. Sag, swell, and momentary interruption signals are obtained by switching on and switching off the load, respectively. The data samples are collected by stepping down the load voltage to 12 V and then converted to digital signal by data acquisition card (DAC) and collected in the PC using the program written in C. The data acquisition system is shown in Fig. 4(a).

Each of the figures contained following plots.

a) Original distorted signal.
b) ST contour plots.
c) Estimated amplitude or frequency.

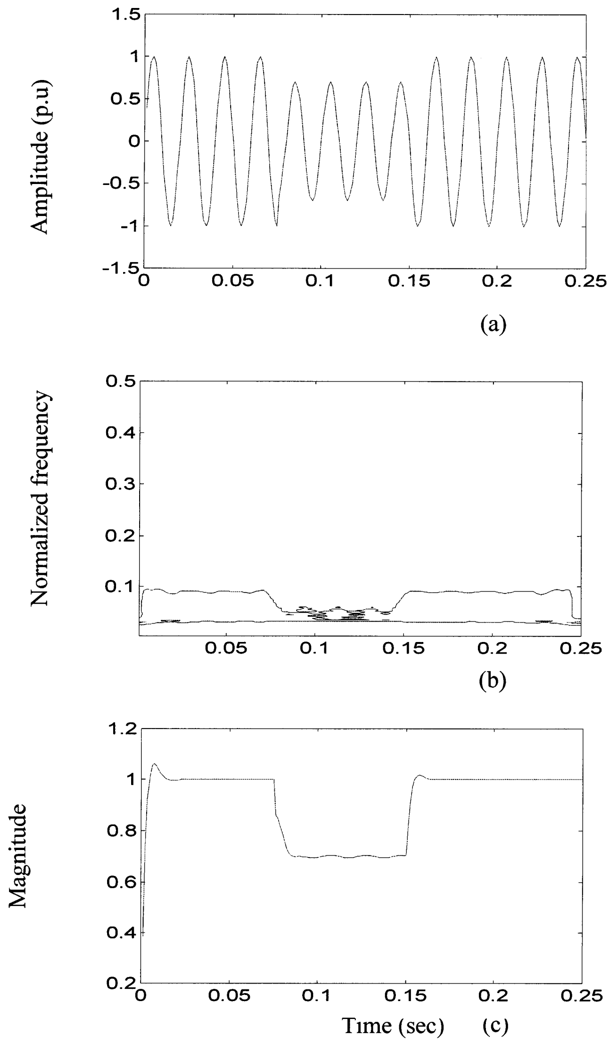

Fig. 7. (a) Example of voltage sag. (b) ST contour plot. (c) Estimated amplitude.

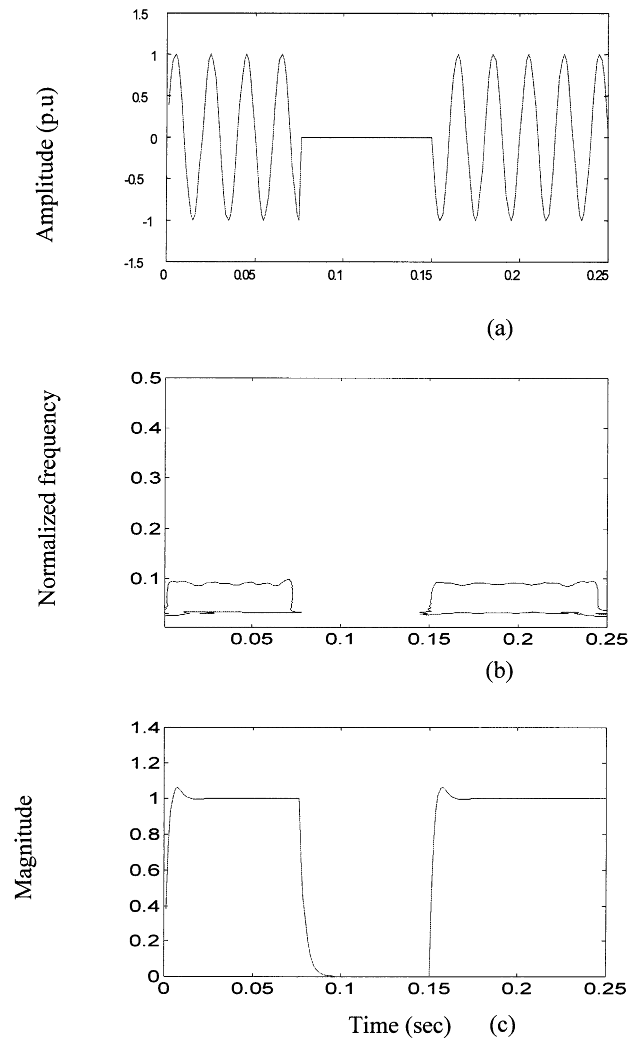

Fig. 8. (a) Example of momentary interruption. (b) ST contour plot. (c) Estimated amplitude.

3) Results From Laboratory Experiment:

a) Voltage Swell: The voltage swell describes the brief increase in the magnitude of the rated system voltage as shown in Figs. 5(a) and 6(a). The hybrid ST and Kalman filtering (HSTKF) approach is applied to this sudden rise of the signal for a short duration. It is observed from the results that the new approach perfectly detects, localizes, classifies, and tracks the amplitude of the signal in the presence of harmonics and noise. Different cases of voltage swell (25% and 45%) are tested here to show the efficacy of the proposed approach. The ST contour plots and the Kalman filter amplitude tracking plots are displayed in Figs. 5(b), 6(b), 5(c), and 6(c), respectively. The tracking error is found to be less than 0.5%.

b) Voltage Sag: In the case of voltage sag, there is a drop of 10 to 90% of the voltage lasting for 0.5 cycle to 1 min, and the cause for the sag can be ascribed to the fault, switching of heavy loads and starting of large motors. Figs. 7(b) and (c) depict the results of the ST contour plot and the Kalman filter amplitude-tracking plot. From the graphs presented in Fig. 7, it is noticed that the present approach clearly detects, localizes, classifies and measures the percentage of sag in the distorted signal. The measurement error is less than 0.5% as observed in the case of swell.

c) Momentary Interruption: A momentary interruption may be seen as a momentary loss of voltage on a power system. Such disturbances describe a drop of 90–100 % of the rated system voltage for a duration of 0.5 cycle to 1 min. Fig. 8(a) shows a waveform of momentary interruption. The ST is used here for detection and classification of the distorted signal. Fig. 8(c) shows the estimated amplitude plot, which indicates that the above fault is a momentary interruption type and is having zero amplitude. From the above results, it is evident that by using an integrated ST and Kalman filter, we can accurately detect, localize, classify, and measure the disturbances of power quality event signals.

V. Conclusion

This paper introduces the use of the ST and Kalman filtering approach as powerful analysis tools that can be used to classify and measure the system response to nonstationary signals. Using the ST alone, one can detect, localize, and visually classify the short duration events in the signal. Then, the Kalman filtering technique is used to extract important features from the analyzed signal, and an integrated ST and EKF approach can classify the nature of the disturbance present in the signal. Further, the EKF accurately tracks the change in amplitude, frequency, phase, and harmonic content of the distorted signal. The method is applied on different sets of data obtained from computer simulations and laboratory tests, and accurate results are obtained in most of the case studies.

REFERENCES

[1] O. Rioul and X. Vetterli, "Wavelets and signal processing," *IEEE Signal Processing Mag.*, pp. 14–38, Oct. 1991.

[2] R. P. Binghom, D. Kreises, and S. Santoso, "Advances in data reduction techniques for power quality instrumentation," in *Proc. Third European Power Quality Con.*, Bremon, Germany, Nov. 1995.

[3] L. Angrisani, P. Daponte, M. D. Apuzzo, and A. Testa, "A new wavelet transform based procedure for electrical power quality analysis," in *Proc. 7th Int. Conf. Harmonics and Quality of Power*, Las Vegas, NV, Oct. 16–18, 1996, pp. 608–614.

[4] P. Pillay, P. Riher, and O. Tag, "Power quality modeling using wavelet," in *Proc. 7th Int. Conf. Harmonics and Quality of Power*, Las Vegas, NV, Oct. 16–18, pp. 625–631.

[5] D. C. Robertson, O. E. Camps, J. S. Mayer, and W. B. Gish, "Wavelet and electromagnetic power system transients," *Trans. Power Delivery*, vol. 11, pp. 1050–1058, Apr. 1996.

[6] S. G. Mallat, "A theory for multiresolution signal decomposition: The wavelet representation," *IEEE Trans. Pattern Anal. Mac. Intell.*, vol. 11, no. 7, pp. 674–693, July 1989.

[7] M. Daubechies, *Ten Lectures in Wavelets*. Philadelphia, PA: Society for Industrial and Applied Mathematics, 1992.

[8] S. Santoso, E. J. Powers, and W. M. Grady, "Power quality disturbance data compression using wavelet transform methods," *IEEE Trans. Power Delivery*, vol. 12, pp. 1250–1257, July 1997.

[9] N. S. Tunaboylu and E. R. Collins, "The wavelet transform approach to detect and quantify voltage sags," in *Proc. 7th Int. Conf. Harmonics and Quality of Power*, Las Vegas, NV, Oct. 16–18, 1996, pp. 619–623.

[10] R. G. Stockwell, L. Mansinha, and R. P. Lowe, "Localization of the complex spectrum: The S-transform," *IEEE Trans. Signal Processing*, vol. 44, pp. 998–1001, Apr. 1996.

[11] A. A. Girgis and T. L. D. Hwang, "Optimal estimation of voltage phasors and frequency deviation using linear and nonlinear Kalman filtering," *IEEE Trans. Power App. Syst.*, vol. 103, pp. 2943–2949, Oct. 1984.

[12] M. S. Sachdev and M. M. Giray, "Off-nominal frequency measurements in electric power systems," *IEEE Trans. Power Delivery*, vol. 4, pp. 1573–1578, June 1989.

[13] P. K. Dash, R. K. Jena, G. Panda, and A. Routray, "An extended complex Kalman filter for frequency measurement of distorted signals," *IEEE Trans. Instrum. Meas.*, vol. 49, pp. 746–-753, Aug. 2000.

[14] O. C. Montero-Hernandez and P. N. Enjeti, "Exploring a low-cost approach to maintaining continuous connections between buildings and/or industrial systems," *IEEE Ind. Applicat. Mag.*, pp. 45–53, Nov./Dec. 2002.

P. K. Dash (SM'90) is a Director with the Silicon Institute of Technology, Bhubaneshwar, India. He was a Professor with the Faculty of Engineering, Multimedia University, Cyberjaya, Malaysia. He was also a Professor of electrical engineering and Chairman, Center for Intelligent Systems, National Institute of Technology, Rourkela, India, for more than 25 years. In addition, he had several visiting appointments in Canada, the U.S., Switzerland, and Singapore. He has published nearly 150 papers in international journals and nearly 100 in international conferences. His research interests are in the area of power quality, FACTS, soft computing, deregulation and energy markets, signal processing, and data mining.

Prof. Dash is a Fellow of the Indian National Academy of Engineering and a Fellow of Institution of Engineers, India.

M. V. Chilukuri (M'01) was born in Visakhapatnam, Andhra Pradesh, India, on May 20, 1972. He received M.E. degree in power systems and automation from the Andhra University, Visakhapatnam. He is currently pursuing the Ph.D.

Since February 2001, he has been a Lecturer with the Faculty of Engineering, Multimedia University, Cyberjaya, Malaysia. His research interests are power quality, time-frequency analysis, soft computing, and corona and partial discharges.

Mr. Chilukuri is currently a member of the Institution of Electrical Engineers, U.K., and a member of the CIGRE Malaysia National Committee.